This article was downloaded by: [Tomsk State University of Control Systems and Radio]
On: 21 February 2013, At: 11:26
Publisher: Taylor & Francis
Informa Ltd Registered in England and Wales Registered Number: 1072954 Registered office: Mortimer House, 37-41 Mortimer Street, London W1T 3JH, UK

Molecular Crystals and Liquid Crystals
Publication details, including instructions for authors and subscription information:
http://www.tandfonline.com/loi/gmcl16

Effects of Electric Fields on the Helical Pitch in Chiral Smectic C Liquid Crystals

D. S. Parmar [a], K. K. Raina [a] & J. Shankar [a]
[a] Department of Physics, University of Kashmir, Srinagar, 190 006, India
Version of record first published: 13 Dec 2006.

To cite this article: D. S. Parmar , K. K. Raina & J. Shankar (1983): Effects of Electric Fields on the Helical Pitch in Chiral Smectic C Liquid Crystals, Molecular Crystals and Liquid Crystals, 103:1-4, 77-98

To link to this article: http://dx.doi.org/10.1080/00268948308071041

PLEASE SCROLL DOWN FOR ARTICLE

Full terms and conditions of use: http://www.tandfonline.com/page/terms-and-conditions

This article may be used for research, teaching, and private study purposes. Any substantial or systematic reproduction, redistribution, reselling, loan, sub-licensing, systematic supply, or distribution in any form to anyone is expressly forbidden.

The publisher does not give any warranty express or implied or make any representation that the contents will be complete or accurate or up to date. The accuracy of any instructions, formulae, and drug doses should be independently verified with primary sources. The publisher shall not be liable for any loss, actions, claims, proceedings, demand, or costs or damages whatsoever or howsoever caused arising directly or indirectly in connection with or arising out of the use of this material.

Mol. Cryst. Liq. Cryst., 1983, Vol. 103, pp. 77–98
0026-8941/83/1034–0077/$18.50/0
© 1983 Gordon and Breach, Science Publishers, Inc.
Printed in the United States of America

Downloaded by [Tomsk State University of Control Systems and Radio] at 11:26 21 February 2013

Effects of Electric Fields on the Helical Pitch in Chiral Smectic C Liquid Crystals

D. S. PARMAR, K. K. RAINA and J. SHANKAR †

Department of Physics, University of Kashmir, Srinagar-190 006 (India).

(*Received January 28, 1983; in final form May 27, 1983*)

Electric fields (d.c. or low frequency a.c.) applied perpendicular to the helical axis interact with the Chiral Smectic C (Sm C*) through coupling of the permanent polarization. The helix pitch increases on the application of electric field and unwinds completely at a critical electric field E_c. We report here the experimental observations on the variation of the helix pitch as a function of temperature in the Sm C* phase and frequency of the applied electric field. E_c required to unwind the helix has been measured for a category of Sm C* liquid crystals having:

1. negative dielectric anisotropy and low permanent polarization,
2. positive dielectric anisotropy and low permanent polarization,
3. positive dielectric anisotropy and higher permanent polarization.

The results have been discussed in the light of the method used by de Gennes to calculate E_c for unwinding the helix in cholesterics and extended to the Sm C* phase by Meyer and Martinot-Lagarde. From these measurements it has been possible to calculate permanent electric polarization in these materials.

1. INTRODUCTION

Ferroelectricity was first discovered in Chiral Smectic C Liquid Crystals (Sm C*) in 1975 by Meyer.[1] Since then extensive studies including the electro-optic, dielectric and electric polarization measurements, have been made on a number of materials by many groups the world over.[2–5] However, the spontaneous polarization in these materials has been observed to be much lower than those in solid ferro-electrics. The

†Department of Chemistry, University of Kashmir, Srinagar-190 006 (India).

Downloaded by [Tomsk State University of Control Systems and Radio] at 11:26 21 February 2013

lower observed spontaneous polarization has been explained on the basis of free rotation of the Chiral Smectic C Liquid Crystal molecules around their long axes and intermolecular rotation and vibration. However, the behaviour of helix in Sm C* under the action of external electric fields is not so well understood, although efforts have been made by certain authors[1,8] to determine the critical electric fields to unwind the helix through polarization and dielectric anisotropy couplings with the electric field. It is known that the parallel stripes are seen under the microscope when the Sm C* is sandwiched between two glass substrates with the helical axis parallel to the plates. The spacings between the stripes give the pitch of the helical structure of these materials. In this paper, experimental observations of the effects of external electric fields (d.c. and low frequency a.c.) on the helix pitch in Sm C* are reported as a function of frequency of the applied electric field and temperature of the sample. Martinot-Lagarde,[6] while calculating the critical electric field required to completely unwind the helix has predicted the determination of spontaneous polarization with the knowledge of the tilt angle θ, helix pitch Z, dielectric anisotropy $\Delta\epsilon$ and the critical electric field E_c for systems having both positive and negative dielectric anisotropies. In the present work spontaneous polarization has been determined using the experimentally determined values of pitch, its electric field dependence and E_c for compounds whose θ and $\Delta\epsilon$ were already known.[7] In section 2, theoretical basis of E_c has been discussed for systems having negative dielectric anisotropy and low permanent polarization, positive dielectric anisotropy and low permanent polarization, and positive dielectric anisotropy and higher permanent polarization. Experimental method and results have been discussed in sections 3 and 4 respectively. Finally the paper has been concluded indicating further investigations which may be undertaken on twist elastic constant K_0 for Sm C* materials studied.

2. THEORY

The determination of critical electric field to unwind the Sm C* helix is based on calculations of Martinot-Lagarde.[6] We consider the Sm C* helix axis along Z, as in Figure 1, and an uniform electric field E applied in the plane of the layers, ϕ being the azimuth angle. If θ is the angle of tilt of the molecule with the helix axis, then the permanent polarization $P_s = P_0\theta$. ϕ is the angle between the permanent polarization and the electric field E. The corresponding free energy density is $-P_0\theta E\cos\phi$. Similarly the free energy density due to the induced

Downloaded by [Tomsk State University of Control Systems and Radio] at 11:26 21 February 2013

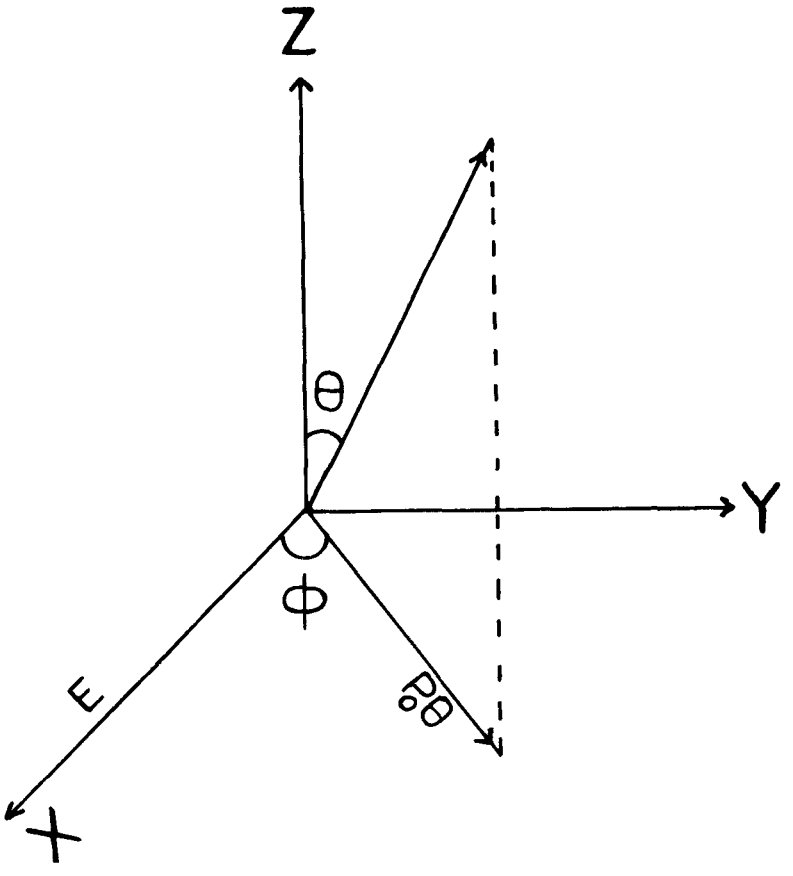

FIGURE 1 Sm C* molecular orientation in an electric field.

polarization is: $-(1/\theta\pi)(\epsilon_\perp E^2 + \Delta\epsilon E_{||}^2)$, where $\Delta\epsilon = \epsilon_{||} - \epsilon_\perp$ is the dielectric anisotropy, $\epsilon_{||}$ and $\epsilon_\perp$ being the two dielectric constants respectively along and perpendicular to the long molecular axis and $E_{||}$ is the component of electric field (E) along the long axis of the dielectric tensor ϵ. An infinite sample along Z in equilibrium will have ϕ dependent part of free energy[6]

$$F = \int_{-\infty}^{+\infty} (1/2) K_0 \theta^2 \left[\left(\frac{\partial \phi}{\partial z} - q_0 \right)^2 + \frac{\Delta\epsilon}{8\pi} E^2 \theta^2 \cos^2\phi - P_0 \theta E \cos\phi \right] dz \tag{1}$$

where $q_0 = 2\pi/Z$. The "flexo" contribution has not been included in

Eq. (1) although some authors[5,8] have preferred to take this into account. The first term in Eq. (1) is the distortion energy for pure twist, the second term represents the contribution due to the coupling with the electric field and the third term the contribution due to permanent polarization.

(*a*) If $\Delta\epsilon < 0$, the induced polarization should help in unwinding the helix in the same way as the permanent polarization. Thus the difference between the free energies of the unwound state and the lower one turn state $[q_0(\partial\phi/\partial z) > 0]$ is[6]

$$\frac{\Delta F}{K_0\theta^2} = -2\pi q_0 + 4\sqrt{\frac{P_0 E}{K_0\theta}}\left(\sqrt{\frac{4\pi P_0}{-|\Delta\epsilon|E\theta}}\sinh^{-1}\sqrt{\frac{|\Delta\epsilon|E\theta}{4\pi P_0}} + \sqrt{1+\frac{|\Delta\epsilon|E\theta}{4\pi P_0}}\right) \tag{2}$$

where $|\Delta\epsilon|$ has been taken as equal to $\epsilon_\perp - \epsilon_\parallel$ for $\Delta\epsilon < 0$.

(*i*) For lower polarization but larger dielectric anisotropy i.e., if $P_0 \approx 0$,

$$2\pi q_0 = 4\sqrt{\frac{|\Delta\epsilon|}{4\pi K_0}} \cdot E_c,$$

or

$$E_c = \frac{\pi^2}{Z}\sqrt{\frac{4\pi K_0}{|\Delta\epsilon|}} \tag{3}$$

(*ii*) For lower dielectric anisotropy but larger polarization i.e., if $\Delta\epsilon$ is negative but $|\Delta\epsilon| \approx 0$

$$2\pi q_0 = 8\sqrt{\frac{P_0 E_c}{K_0\theta}},$$

or

$$E_c = \frac{\pi^4}{4}\frac{K_0\theta}{P_0 Z^2} \tag{4}$$

Eq. (4) represents the critical electric field obtained by Meyer[10] for Sm C* but with the elastic term approximation by Martinot-Lagarde.[6] This equation gives $E_c \propto q_0^2\theta$ by using $Z = 2\pi/q_0$. However, for the observed θ dependence near T_c^* (the Sm C*–Sm A transition temperature), E_c should be smaller than this proportionality.

Downloaded by [Tomsk State University of Control Systems and Radio] at 11:26 21 February 2013

Downloaded by [Tomsk State University of Control Systems and Radio] at 11:26 21 February 2013

TABLE I

Molecular structure, phase transition temperatures and dielectric anisotropies of the compounds studied

Compounds and name	Phase transition temperatures
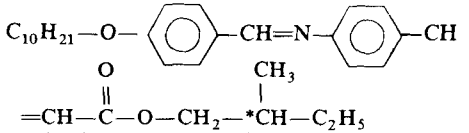 *p*-decyloxybenzylidene *p'*-amino 2-methyl butyl cinnamate (DOBAMBC) $\Delta\epsilon = 2.4$	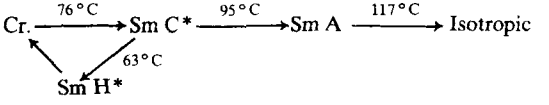
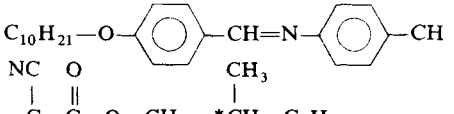 *p*-decyloxybenzylidene *p'*-amino 2-methyl butyl α cyano cinnamate (DOBAMBCC) $\Delta\epsilon = -0.95$	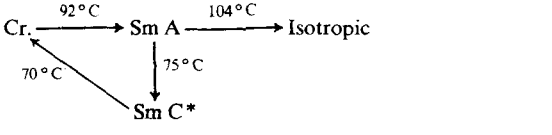
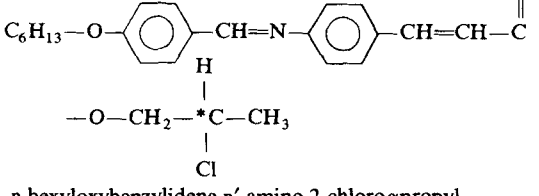 *p*-hexyloxybenzylidene *p'*-amino 2-chloro α propyl cinnamate (HOBACPC) $\Delta\epsilon = 2.95$	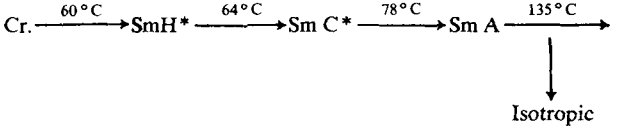

(*b*) If $\Delta\epsilon > 0$, for the case of lower induced polarization, i.e. $K_0\theta^2 q_0^2 \Delta\epsilon/(4\pi P_0^2) \ll 1$, it can be shown that E_c has the same form as Eq. (4) for smaller θ.

For larger induced polarization i.e., $K_0\theta^2 q_0^2 \Delta\epsilon/(4\pi P_0^2) \gg 1$, the free energy is the sum of the energies of the one turn state and the lower energy unwound state corresponding to $\phi = \phi_0$ with $\cos\phi_0 = 4\pi P_0\theta/\Delta\epsilon\theta^2 E_c$. Therefore,[6] for larger permanent polarization,

$$E_c = \frac{\pi^2 K_0 \theta q_0^2}{16 P_0}\left[1 + \frac{\pi^2}{48} \cdot \frac{K_0\theta^2 q_0^2 \Delta\epsilon}{4\pi P_0^2}\right] \tag{5}$$

Comparison of Eqs. (4) and (5) reveals that E_c is larger for compounds with $\Delta\epsilon > 0$ than for those with $\Delta\epsilon < 0$. This is because the induced polarization in case $\Delta\epsilon > 0$ hinders the unwinding due to permanent polarization.

3. EXPERIMENTAL

The compounds studied were synthesized by P. Keller and C. Germain at Orsay, France. Their molecular structure, phase transition temperatures, dielectric anisotropies and abbreviated names are given in Table I. The compounds were purified several times by recrystallization from ethanol solution. The samples were sandwiched between two SnO_2 coated glass plates on which a thin semiconducting layer of SiO was vacuum evaporated at an oblique incidence. The SnO_2 coating acted as electrodes through which electric fields were applied. Mylar spacers were used in order to define the thickness of the sample. Homogeneous (planar) orientation was obtained by cooling the sample slowly from isotropic phase to Sm A and then to Sm C*. The planar orientation was, sometimes, also encouraged by application of a low frequency ($\approx$ 10–20 Hz) voltage ($\approx$ 20–200 V m s) between the electrodes while cooling the sample from isotropic to Sm A phase. Finger print pattern observed under the microscope corresponding to planar orientation in Sm C* phase is shown in Figure 2. The sample temperature was maintained to better than 0.1°C with the help of a Mettler FP_5 and FP_{52} hot stage which could be mounted on an optical microscope stage to observe visually the electric field effects. The helix pitch was measured using optical microscope by counting the number

Downloaded by [Tomsk State University of Control Systems and Radio] at 11:26 21 February 2013

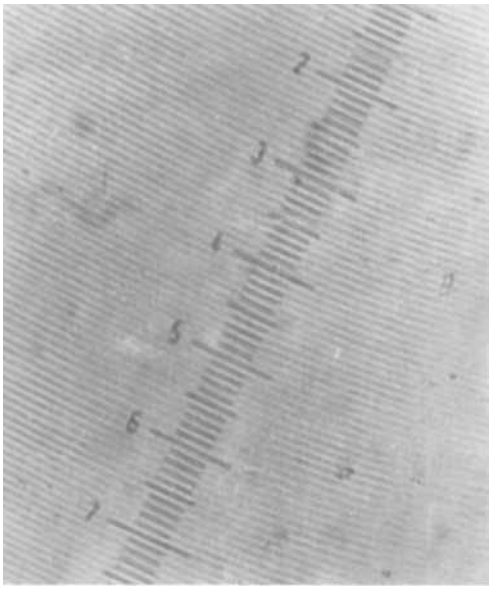

FIGURE 2 Sm C* domain texture in planar orientation and helix pitch measurements.

of stripes in a 50 μm distance under the microscope with the help of a calibrated graticule as shown in Figure 2. The same procedure was adopted for the electric field effect on helix pitch. The counting of the stripes was done at three different regions of the sample and an average value of the pitch was considered. The Sm A–Sm C* transition temperature T_c* was the temperature at which we observed colours and stripes under the optical microscope due to formation of helix when the temperature was lowered slowly from Sm A to Sm C* phase. The stripes and colours disappeared at the same temperature when it was increased slowly from Sm C* to Sm A phase.

4. RESULTS AND DISCUSSION

4.1 Temperature dependence of helix pitch

The pitch and its temperature dependence for all the three compounds have been studied. Typical temperature dependence for HOBACPC is shown in Figure 3. A striking feature is the decrease of helix pitch near T_c* in agreement with the general observations with other Sm C*

Downloaded by [Tomsk State University of Control Systems and Radio] at 11:26 21 February 2013

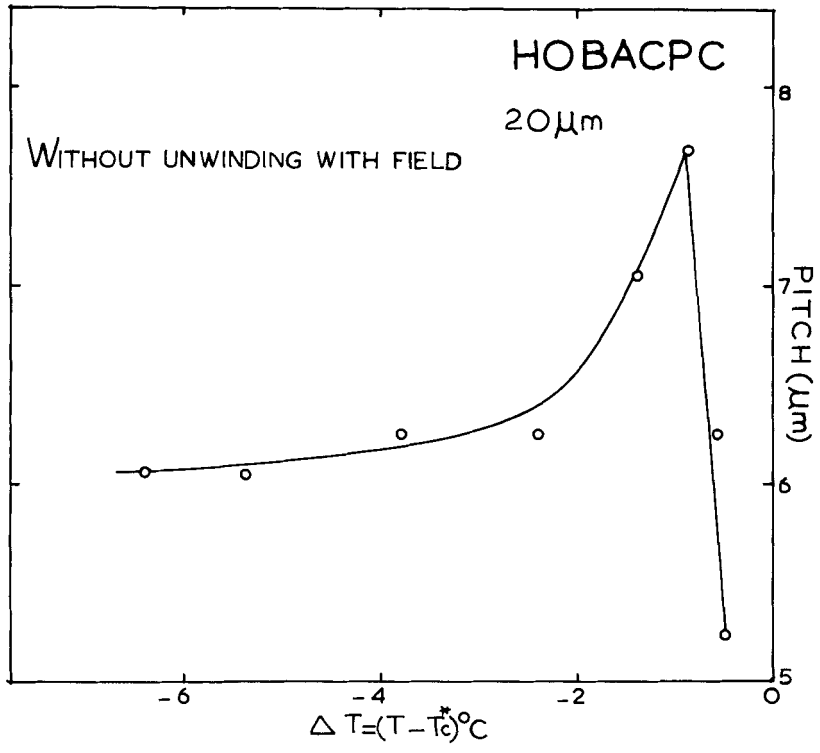

FIGURE 3 Temperature dependence of helix pitch in HOBACPC.

compounds. No theoretical model is available to explain the temperature dependence of the pitch. However, Pikin[11] has shown, by minimization of free energy F with respect to q_0 at $\theta(Z) = \theta_0$ = constant and $\phi(Z) = \phi_0(Z) = q_0 Z$, that the pitch has no singular temperature dependence and is finite at T_c^*.

4.2 Electric field effects on the helix pitch

If an electric field is applied to the Sm C* phase parallel to the smectic layers, the induced and permanent polarizations distort the helicoidal structure. The helix pitch increases with the electric field and disappears completely at some critical field E_c. In this situation the polarization is unwound and helix becomes infinite. The sample comes to an ordinary Sm C phase at E_c which is a function of temperature.

4.2.1 D.C. field effects. Typical behaviours of the helix pitch with d.c. electric fields at various temperatures in DOBAMBC ($\Delta\epsilon$ = 2.4)

Downloaded by [Tomsk State University of Control Systems and Radio] at 11:26 21 February 2013

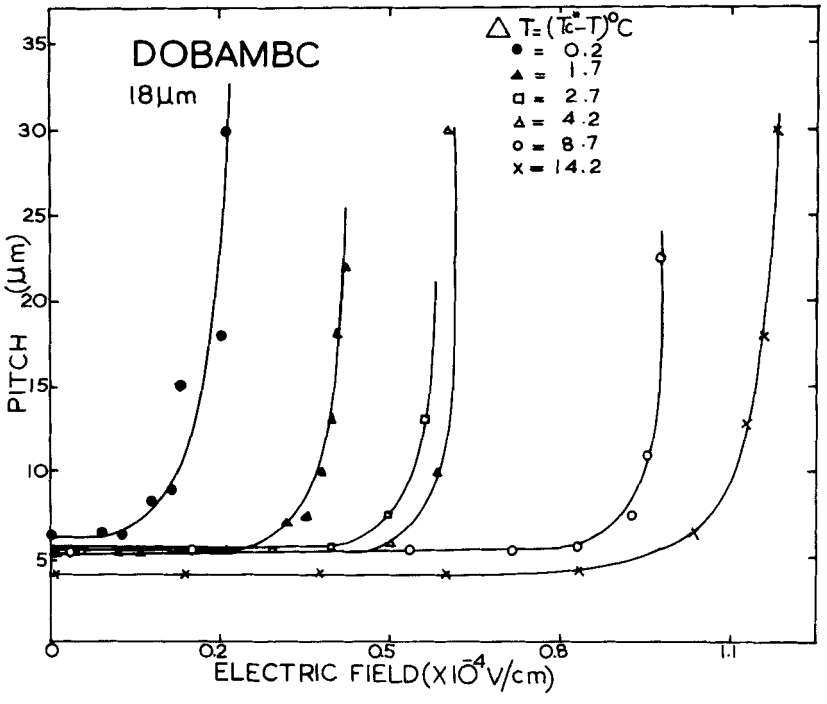

FIGURE 4(a) d.c. electric field effect on helix pitch in DOBAMBC at different temperatures in Sm C* phase.

and DOBAMBCC ($\Delta\epsilon = -0.95$) are shown in Figure 4(a, b). The sample thickness was 18 μm. In both cases, the helix pitch increases with increase in electric field ($\approx 10^3$ V/cm). At lower values of the field, there is practically no change in pitch. The pitch suddenly unwinds and tends to become infinite near E_c. The dispersion in pitch for $E = 0$ corresponds to the general temperature dependence of the pitch for these compounds. It is interesting to note that at the same distance from T_c^* ($\Delta T = T_c^* - T = 1.7\,^\circ$C) the helix unwinds and the pitch becomes infinite at a lower value of electric field ($E_c \approx 0.48 \times 10^4$ V/cm) in DOBAMBCC ($\Delta\epsilon < 0$) than in DOBAMBC ($\Delta\epsilon > 0$) where the helix pitch tends to become infinite at $E_c \approx 1.2 \times 10^4$ V/cm. This can be explained on the basis of the theory discussed in section 2 for compounds having positive and negative dielectric anisotropies. DOBAMBC having $\Delta\epsilon = 2.4$, has larger value of E_c since the induced polarization in it hinders the unwinding due to the permanent polarization. The same is the case for HOBACPC ($\Delta\epsilon = 2.95$). On the

Downloaded by [Tomsk State University of Control Systems and Radio] at 11:26 21 February 2013

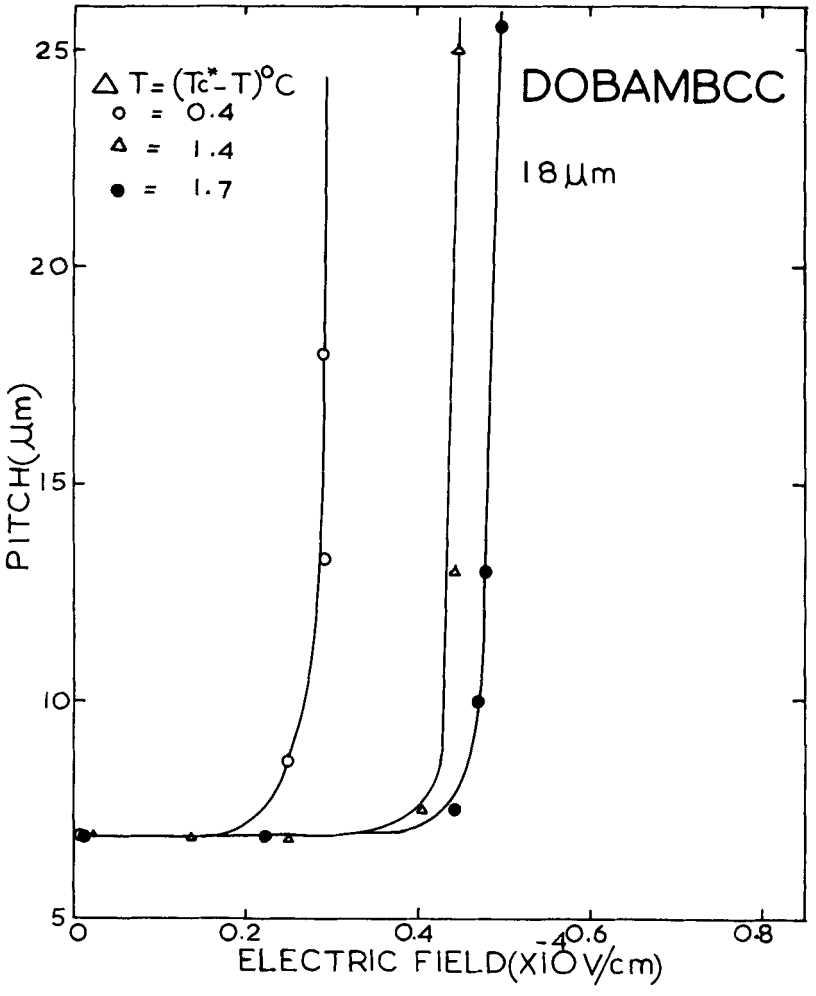

FIGURE 4(b) d.c. electric field effect on helix pitch in DOBAMBCC at different temperatures in Sm C* phase.

other hand in DOBAMBCC ($\Delta\epsilon = -0.95$), the induced polarization helps to unwind the helix and give the same unwound state as the permanent polarization ($\phi = 0$).

The critical electric field E_c required to unwind the helix has been taken as the point on E-axis where the pitch becomes infinite and disappears completely. This was ascertained visually in the microscope for DOBAMBC, DOBAMBCC and HOBACPC. The E_c measurements as function of temperature in the Sm C* phase are shown in

Downloaded by [Tomsk State University of Control Systems and Radio] at 11:26 21 February 2013

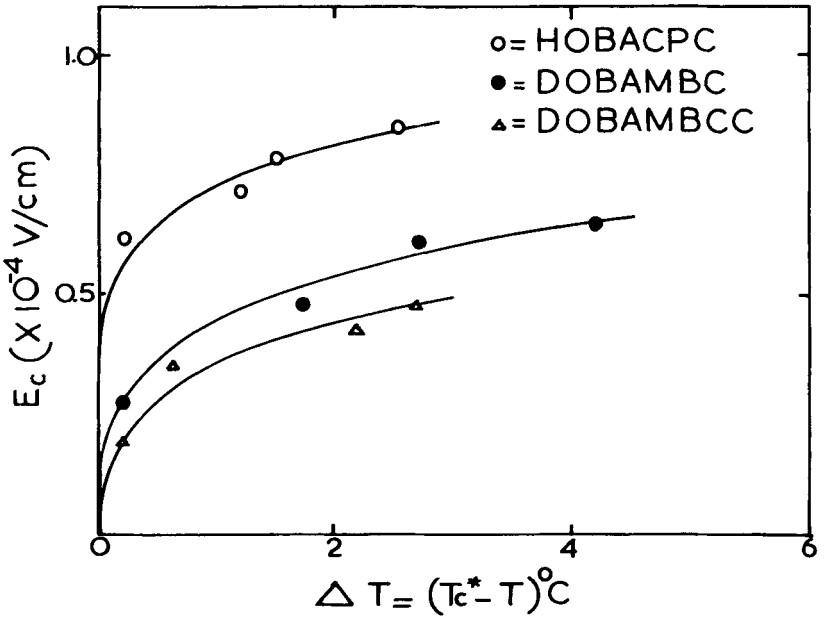

FIGURE 5 d.c. critical field, E_c, required to unwind the helical structure in DOBAMBC, HOBACPC and DOBAMBCC. The solid lines are theoretical fits.

Figure 5. The solid lines correspond to theoretical plots of E_c from Eqs. (4) and (5) for DOBAMBC and HOBACPC respectively (both have $\Delta\epsilon > 0$) and from Eq. (3) for DOBAMBCC ($\Delta\epsilon < 0$). The theoretical calculations very well agree with the experimental results for $K_0 = 0.5 \times 10^{-6}$ C.G.S., 0.9×10^{-6} for C.G.S. and 0.2×10^{-6} C.G.S. respectively for DOBAMBC, HOBACPC and DOBAMBCC. The θ and P_0 values required for theoretical calculations have been taken from previous measurements.[2,12] It is interesting to note that E_c for the same ΔT (Figure 5) is lowest for DOBAMBCC ($\Delta\epsilon < 0$) and highest for HOBACPC ($\Delta\epsilon > 0$). HOBACPC has larger (about 5 times) permanent polarization ($P_0 = 0.05$ Debye/mol. rad. for the chloro-group at chiral atom) than DOBAMBC ($P_0 = 0.01$ Debye/mol. rad. for methyl group at the chiral atom). HOBACPC thus would also possess larger value of induced polarization. The weak temperature dependence of E_c far from T_c^* can be explained as due to the small P_0 dependence on T from the 'flexo' contribution. Also it will be seen that near T_c^* ($\Delta T \approx 0$), E_c is larger than proportional to $q_0^2\theta$ both for DOBAMBC and HOBACPC ($\Delta\epsilon > 0$) and slightly smaller than proportional to $q_0^2\theta$ for DOBAMBCC ($\Delta\epsilon < 0$) in agreement with theory

Downloaded by [Tomsk State University of Control Systems and Radio] at 11:26 21 February 2013

(section 2). This is because at a temperature T defined by $\theta^2(T)q_0^2(T)\Delta\epsilon/(4\pi P_0^2) = 1$, the unwound state no longer corresponds to $\phi = 0$ but to $\phi = \phi_0$ with $\text{Cos}\,\phi_0 = 4\pi P_0\theta/\Delta\epsilon\theta^2 E$.

4.2.2. A.C. field effects. The question of dynamics of Sm C* helix under a.c. electric fields is still an unsolved problem although efforts have been made by Ostrovskii *et al.*[4] to explain it by considering the dynamic viscosity effects in the free energy calculations. Introduction of the term $-\gamma\theta(d\phi/dt)$ (where γ is the dynamic viscosity coefficient) in Eq. (1) for free energy under an a.c. electric field $E = E_0 e^{i\omega t}$ and the similar calculations for E_c, as discussed in section 2, indicate higher E_c values for a.c. fields than for d.c. fields. The low frequency (20–200 Hz) field effects on helix pitch have been studied in these investigations. The typical dependence of helix pitch on a.c. field at various frequencies is shown in Figure 6 for DOBAMBC ($\Delta T = 2.7\,°C$) and in Figure 7(a, b) for DOBAMBCC at two different ΔT (1.2 °C and 2.2 °C respectively). The pitch increases with a.c. field in both cases.

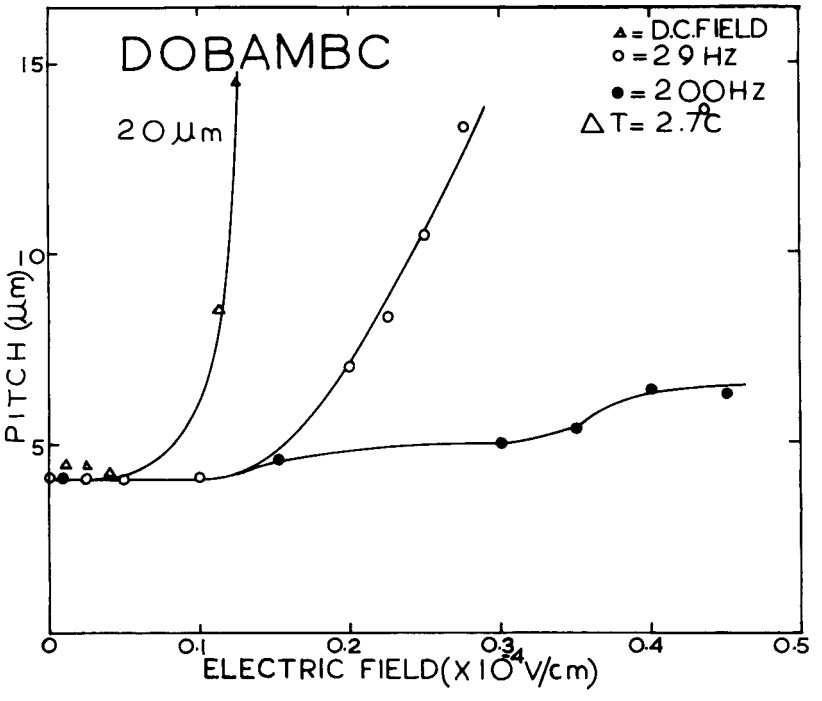

FIGURE 6 a.c. electric field effect on helix pitch for DOBAMBC as function of frequency at $\Delta T = 2.7\,°C$.

Downloaded by [Tomsk State University of Control Systems and Radio] at 11:26 21 February 2013

Downloaded by [Tomsk State University of Control Systems and Radio] at 11:26 21 February 2013

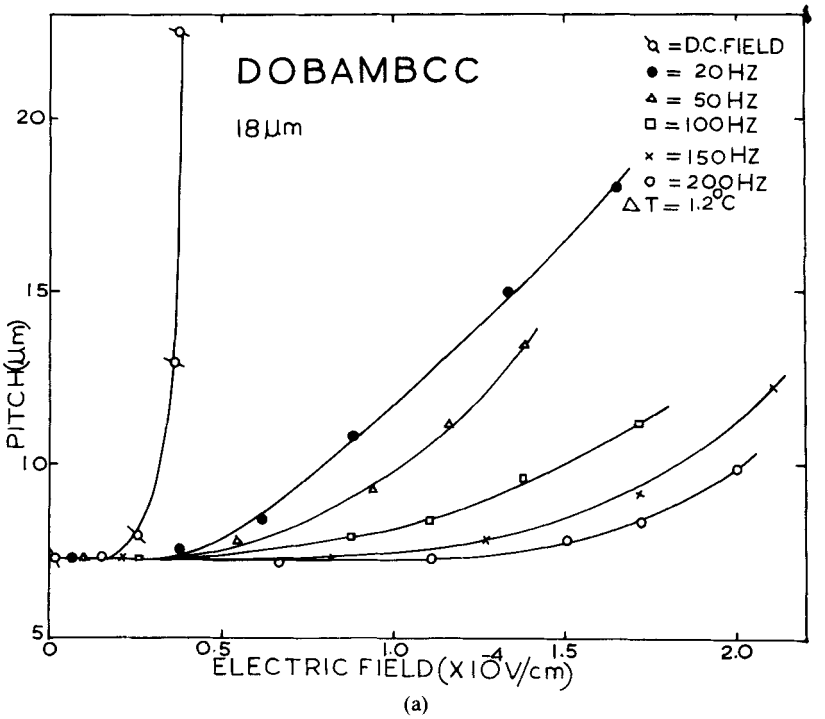

(a)

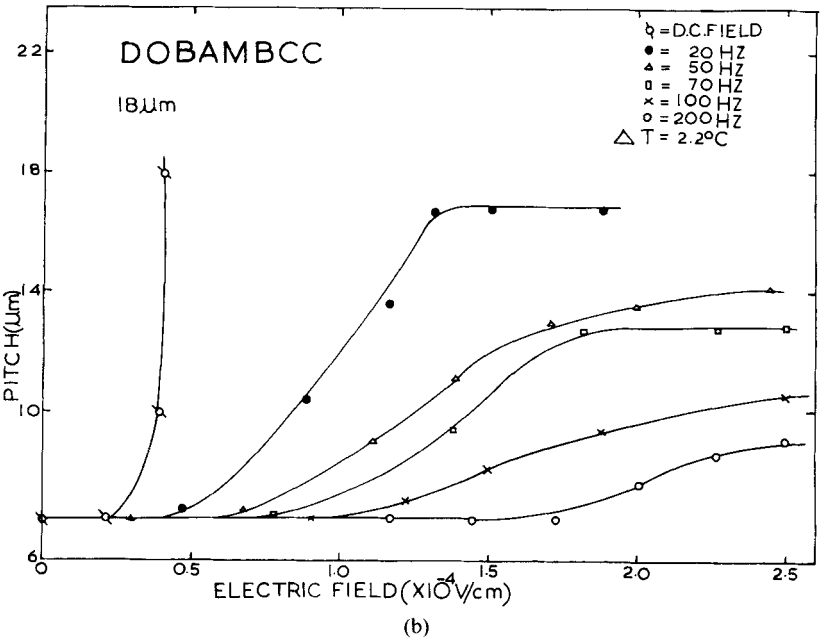

(b)

FIGURE 7 (a) a.c. electric field effect on helix pitch for DOBAMBCC as function of frequency at $\Delta T = 1.2°C$. (b) a.c. electric field effect on helix pitch for DOBAMBCC as function of frequency $\Delta T = 2.2°C$.

The magnitude of actual increase in pitch depends on the frequency of the field.

DOBAMBC. As shown in Figure 6, the pitch diverges at lower fields for d.c. than for a.c. Also, as the frequency increases, the pitch variation with electric field goes on decreasing. At 29 Hz, the pitch tends to diverge at lower fields than at 200 Hz. In fact, at higher frequencies, the E_c required is extremely high. This is due to the fact that the induced polarization is predominant and prevents the helix unwinding. It is interesting to note that both for a.c. and d.c. fields, the pitch does not change appreciably at lower fields. This is because of the coupling of permanent polarization with the electric field.

DOBAMBCC. The pitch dependence with a.c. electric field at various frequencies for DOBAMBCC is shown in Figure 7(a, b) at two different temperatures ($\Delta T = 1.2°C$ and $2.2°C$ respectively). Whereas the general observations on pitch dependence on frequency of the field at $\Delta T = 1.2°C$ are almost similar to those in DOBAMBC, the be-

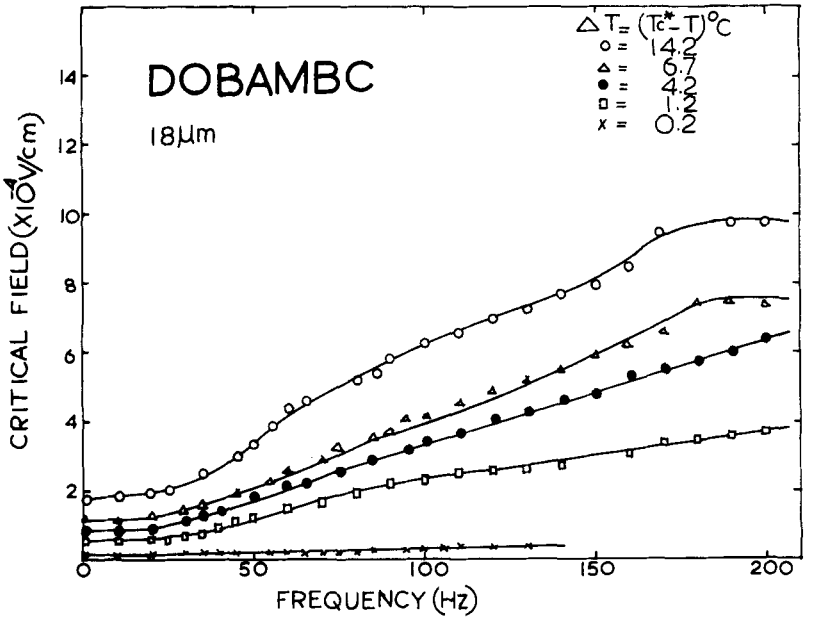

FIGURE 8(a) a.c. critical field as a function of frequency for DOBAMBC at different temperatures in Sm C* phase.

Downloaded by [Tomsk State University of Control Systems and Radio] at 11:26 21 February 2013

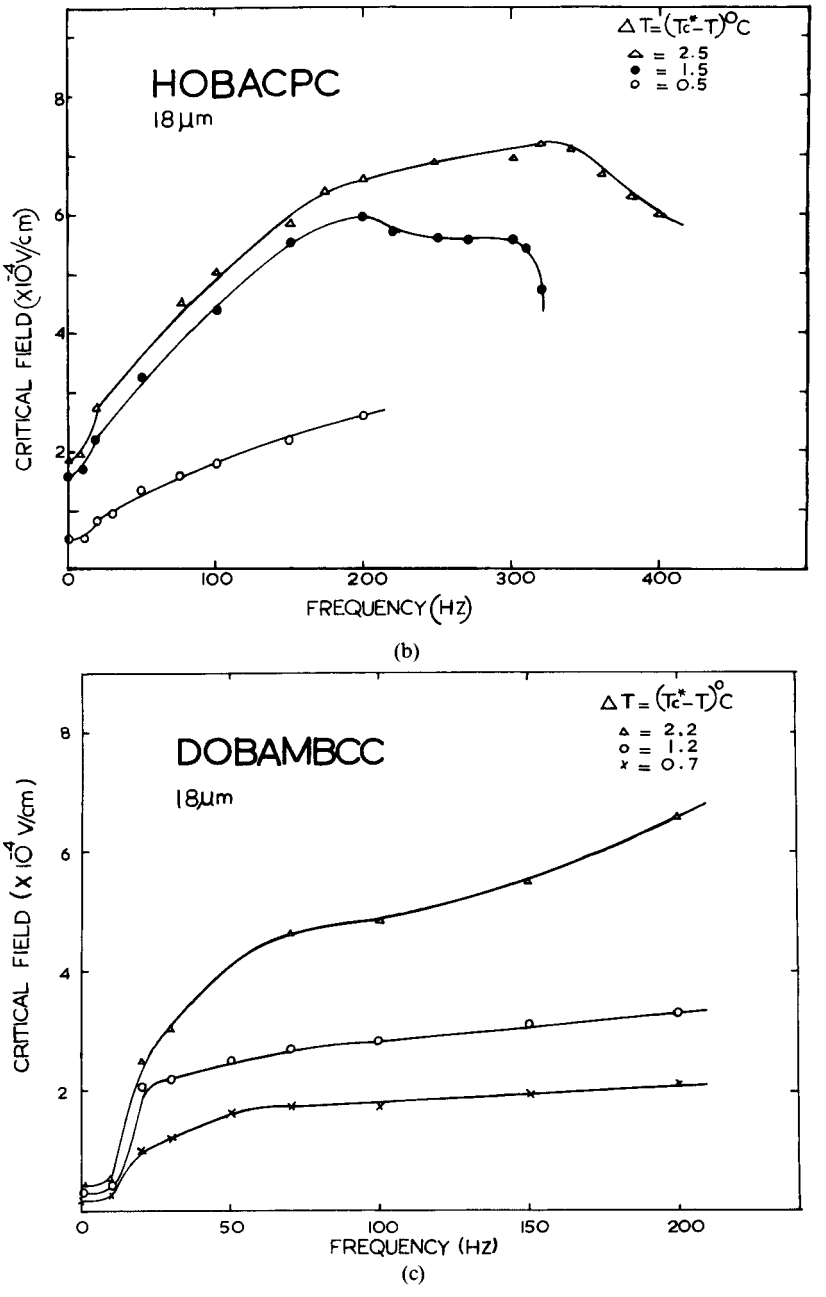

FIGURE 8(b) a.c. critical field as a function of frequency for HOBACPC at different temperatures in Sm C* phase. (c) a.c. critical field as a function of frequency for DOBAMBCC at different temperatures in Sm C* phase.

Downloaded by [Tomsk State University of Control Systems and Radio] at 11:26 21 February 2013

haviour at lower temperature $\Delta T = 2.2°C$ is different at higher values of the electric field. The effects of lower frequency fields are more pronounced at both the temperatures. The inertia of the pitch to a.c. field increases with frequency. For example, for $\Delta T = 1.2°C$ (Figure 7a), the pitch remains at a value of 7.5 μm at d.c. fields up to 2.0×10^3 V/cm and then suddenly diverges at $E = 3.2 \times 10^3$ V/cm. At 20 Hz field, pitch maintains its value of 7.5 μm up to $E = 4.5 \times 10^3$ V/cm and increases slowly beyond it to diverge at $E_c = 1.6 \times 10^4$ V/cm. At 200 Hz, the pitch remains constant at 7.5 μm up to 1.1×10^4 V/cm and starts increasing slowly with the field to diverge at $E_c = 3.4 \times 10^4$ V/cm. However, at lower temperatures ($\Delta T = 2.2°C$) as in Figure 7(b), although the d.c. field behaviour is similar to that at $\Delta T = 1.2°C$, the pitch tends to saturate at higher a.c. fields. For example, at 20 Hz, the pitch saturates beyond $E = 1.2 \times 10^4$ V/cm. The a.c. field beyond which the pitch gets saturated increases

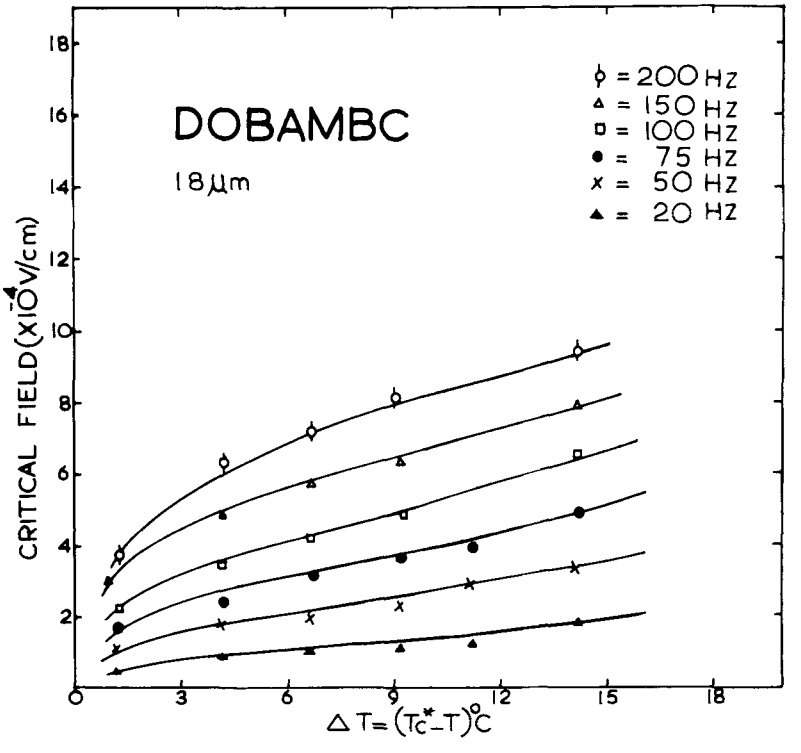

FIGURE 9(a) a.c. critical field as a function of temperature for DOBAMBC in Sm C* phase at different frequencies.

Downloaded by [Tomsk State University of Control Systems and Radio] at 11:26 21 February 2013

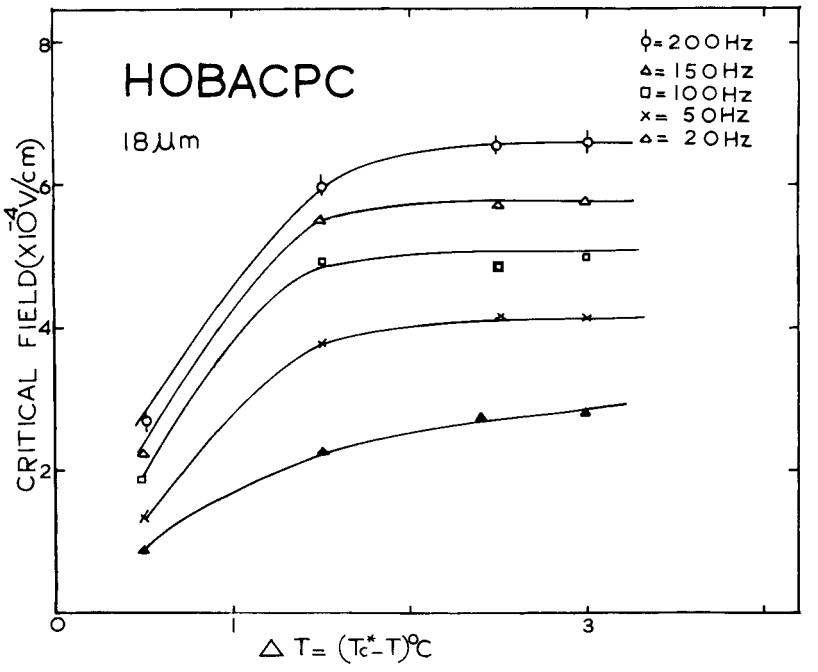

FIGURE 9(b) a.c. critical field as a function of temperature for HOBACPC in Sm C* phase at different frequencies.

with frequency. The competition between induced polarization and dielectric couplings with the applied electric field is responsible for this type of behaviour of the helix pitch in Sm C* under applied a.c. electric fields.

The E_c at different frequencies was taken as the field at which the helix pitch completely unwinds and disappears as seen in the field of the optical microscope. The E_c thus obtained as a function of frequency at various temperatures is shown in Figure 8(a) for DOBAMBC, 8(b) for HOBACPC and 8(c) for DOBAMBCC. E_c increases with frequency of the applied electric field. However, towards lower frequencies, E_c variations are not appreciable. E_c does not change between 0–10 Hz for all these compounds. This is because the permanent polarization can follow such lower frequency fields. However, beyond these frequencies, E_c starts increasing suddenly with frequency. The increase is rapid for 15–50 Hz. This is also the order of the frequency of relaxation for these materials as confirmed by dielectric and conductivity measurements. E_c tends to saturate at higher frequencies due to

Downloaded by [Tomsk State University of Control Systems and Radio] at 11:26 21 February 2013

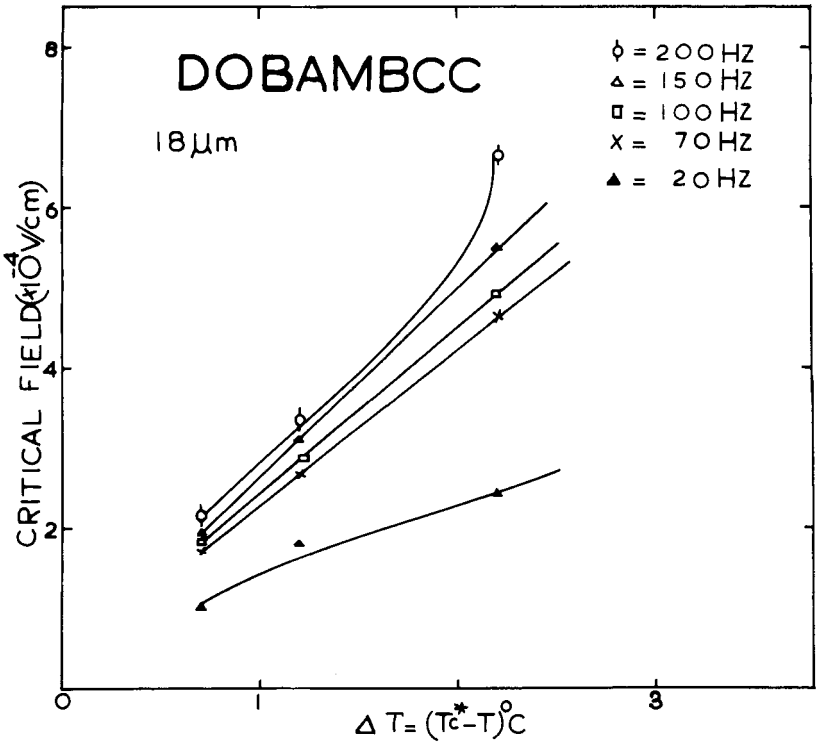

FIGURE 9(c) a.c. critical field as a function of temperature for DOBAMBCC in Sm C* phase at different frequencies.

the dominance of induced polarization effects. It is interesting to note that at a particular frequency of the electric field and at a given temperature of the sample, E_c is highest for HOBACPC (Figure 8b) and lowest for DOBAMBCC (Figure 8c) among the compounds studied. This can be explained on the basis of the permanent polarization and the dielectric anisotropy values for these compounds. HOBACPC has the highest P_0 and $\Delta\epsilon(+ve)$ among the three compounds. The induced polarization hinders the helix unwinding thereby increasing E_c. Similarly DOBAMBC falls next to HOBACPC and thus lower E_c values. DOBAMBCC having negative $\Delta\epsilon$, the induced polarization encourages helix unwinding giving still lower values of E_c in comparison to DOBAMBC. The lower a.c. E_c at higher frequencies and ΔT for HOBACPC (Figure 8b) is expected due to the presence of certain instabilities at higher fields. The same behaviour is reflected in Figure 9(a, b, c) where a.c. E_c has been plotted as a function of $\Delta T = (T_c^* - T)$ for DOBAMBC (Figure 9a), HOBACPC (Figure 9b)

Downloaded by [Tomsk State University of Control Systems and Radio] at 11:26 21 February 2013

and DOBAMBCC (Figure 9c). In all these cases, E_c tends to zero at $\Delta T = 0\,^{\circ}C$, i.e., at T_c^*. Also E_c changes are more rapid near T_c^* at all frequencies. This is due to the $q_0^2\theta$ dependence of E_c in Sm C* as discussed above.

The saturation behaviour of the a.c. E_c at higher frequencies for HOBACPC (Figure 9b) is due to the dielectric anisotropy and ferroelectric couplings with the electric field.

4.3 Calculation of Permanent Polarization

From the above measurements of q_0 and E_c and their temperature dependence, it has been possible to calculate $P_s = P_0\theta$ for these

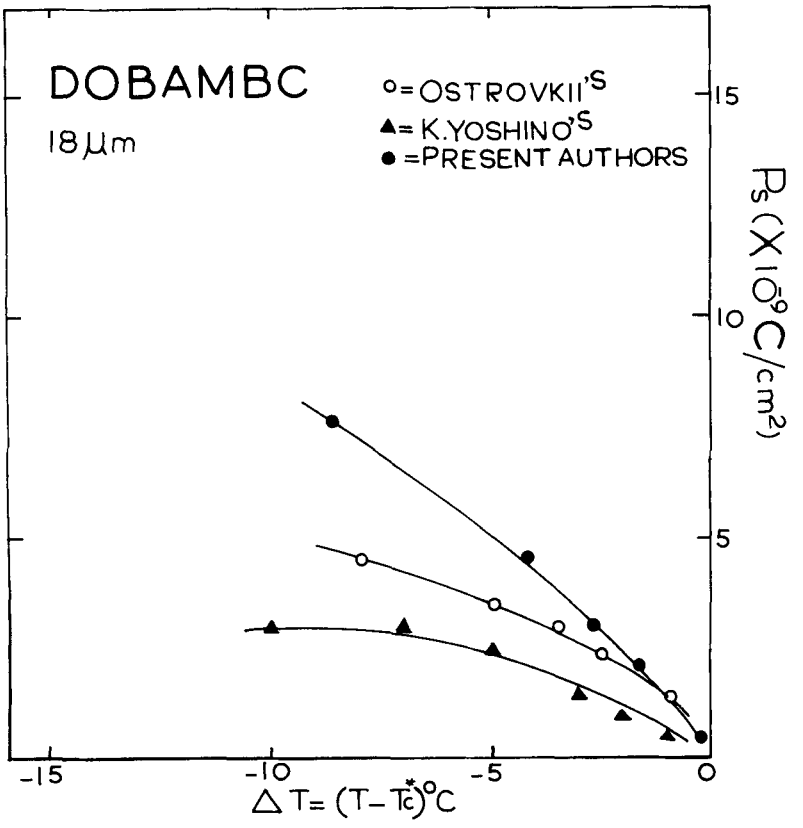

FIGURE 10(a) Calculated (●) and experimental (○, ▲) polarization variation with temperature for DOBAMBC.

Downloaded by [Tomsk State University of Control Systems and Radio] at 11:26 21 February 2013

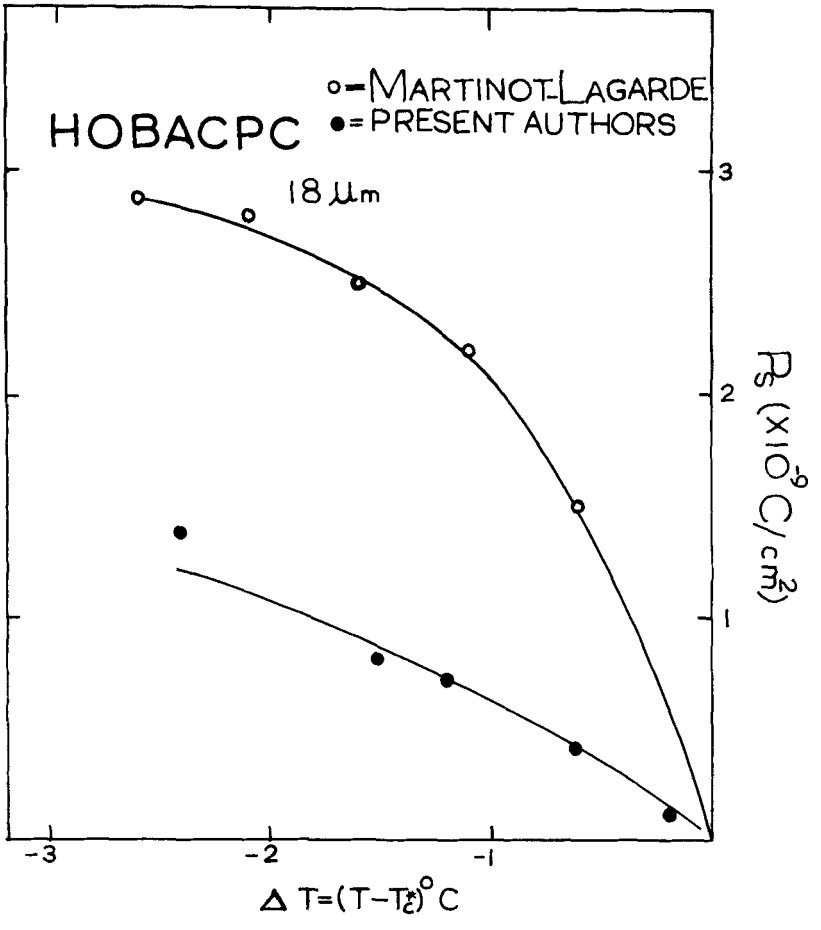

FIGURE 10(b) Calculated (●) and experimental (○) polarization variation with temperature for HOBACPC.

compounds with the help of Eqs. (4) and (5), using previous measurements on θ and $\Delta\epsilon$. The P_s values thus obtained have been shown in Figure 10(a, b, c) for DOBAMBC, HOBACPC and DOBAMBCC as function of temperature (ΔT) in the Sm C* phase. The P_s values from present calculations have been compared with values obtained by direct electrical measurements by other authors.[2,13] For DOBAMBC, (Figure 10a), at temperatures near T_c^* ($\Delta T \approx 0$), the agreement in the experimental values of P_s by Ostrovskii *et al.*[4] and Yoshino *et al.*[13] is fair. However, our calculated values are higher in comparison to the experimental values away from T_c^*. This seems to be partially because Eq. (5), by which P_s has been calculated, is valid for smaller θ.

Downloaded by [Tomsk State University of Control Systems and Radio] at 11:26 21 February 2013

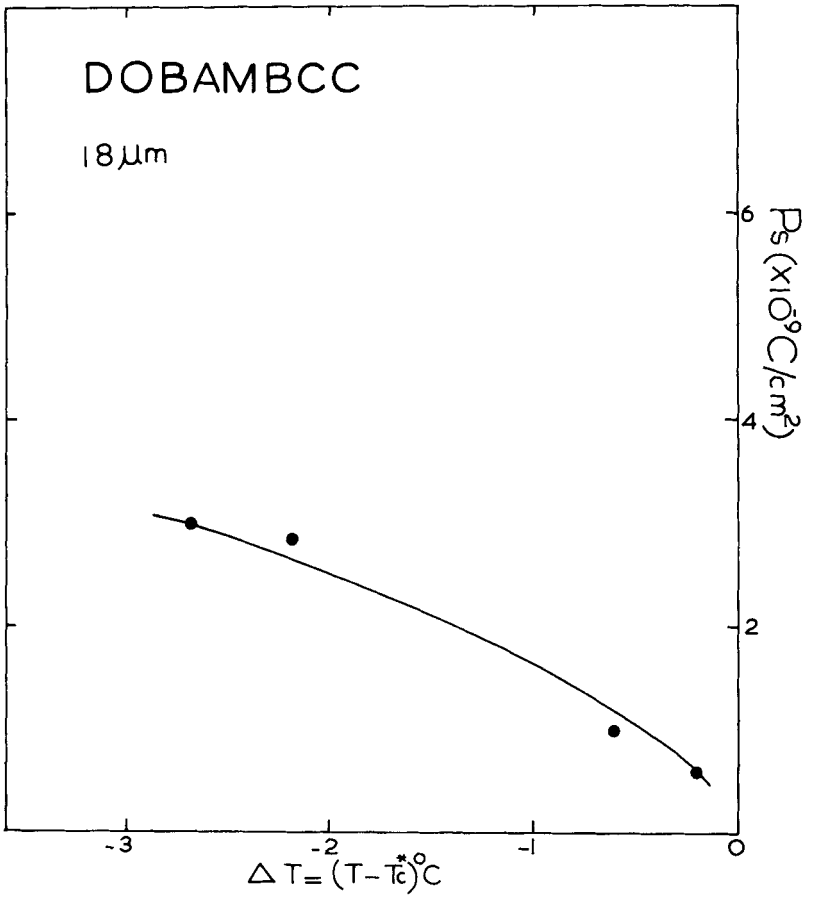

FIGURE 10(c) Calculated polarization (●) for DOBAMBCC.

In the case of HOBACPC (Figure 10b), our calculated values of P_s are much lower than those obtained by direct electrical measurements by Martinot-Lagarde.[3] It seems that the sample used by Martinot-Lagarde was impure and ionic presence contributed towards the total measured charge from which the absolute polarization was determined. This is also evident from the Sm C*–Sm A transition temperature reported for the sample. However, the exact value of the elastic constant and its temperature dependence might also be responsible for the lower calculated values from the present experiments. The K_0 value used in the calculations has been taken to be 0.9×10^{-6} C.G.S.

The P_s behaviour with temperature for DOBAMBCC (Figure 10c) is also the same as for DOBAMBC and HOBACPC. However, in

Downloaded by [Tomsk State University of Control Systems and Radio] at 11:26 21 February 2013

absence of any experimental results on this compound, the P_s values obtained from present method could not be compared.

3. CONCLUSIONS

1. The critical field E_c required to unwind the helix has been measured experimentally by measuring the helix pitch variation with applied electric field (both d.c. and a.c.). The d.c. E_c results for DOBAMBC, HOBACPC and DOBAMBCC are in perfect agreement with the theoretical predictions of Martinot-Lagarde.[6]

2. The a.c. E_c effects on helix pitch have been experimentally studied. The a.c. E_c values are higher in comparison to d.c. E_c values for all the three compounds. There is still no theory for a.c. E_c calculations to compare the experimental results.

3. The polarization P_s has been calculated from experimental measurements of θ, q_0, $\Delta\epsilon$ and E_c. The results are in agreement with the predictions of Martinot-Lagarde.[6] However, experimental measurements on K_0 are needed to explain the experimental results.

4. The frequency dependence of E_c is less well understood and the anomalies in the high frequency regime observed in HOBACPC (Figure 8b), are still to be explained.

Acknowledgments

The authors are grateful to Martinot-Lagarde and G. Durand for many helpful discussions. They are also grateful to P. Keller and C. Germain for synthesizing the samples. The interest of M. K. Khera in these investigations is thankfully acknowledged.

References

1. R. B. Meyer, L. Liebert, L. Strzelecki and P. Keller, *J. Phys. Lett.* (*Paris*), **36**, L69 (1975).
2. Ph. Martinot-Lagarde, *J. Phys. Lett.*, **38**, L17 (1977).
3. S. Garoff and R. B. Meyer, *Phys. Rev.*, **A-19**, 388 (1979).
4. B. I. Ostrovskii, A. Z. Rabinovich, A. S. Sonin, and B. A. Strukov, *Sov. Phys. JETP*, **45**, 912 (1978).
5. R. Blinc and B. Zeks, *Phys. Rev.*, **A-18**, 740 (1978).
6. Ph. Martinot-Lagarde, *Mol. Cryst. Liq. Cryst.*, **66**, 61 (1981).
7. D. S. Parmar and Ph. Martinot-Lagarde, *Ann. Phys.*, **3**, 275, (1978).
8. S. A. Pikin and V. L. Indenbom, *Sov. Phys. Usp.*, **21**, 487 (1978).
9. P. G. de Gennes, *The Physics of Liquid Crystals*, Clarendon Press, (1974).
10. R. B. Meyer, *Mol. Cryst. Liq. Cryst.*, **C-40**, 33 (1977).
11. S. A. Pikin, *Liquid Crystals*, Heyden, London, 1980.
12. Ph. Martinot-Lagarde, *J. Phys.* (*Paris*), **37**, C3-129 (1976).
13. K. Yoshino, T. Uemoto and Y. Inushi, *Jap. J. Appl. Phys.*, **16**, 571 (1977).

Downloaded by [Tomsk State University of Control Systems and Radio] at 11:26 21 February 2013